International Journal on Science and Technology (IJSAT)
E-ISSN: 2229-7677 ● Website: www.ijsat.org ● Email: editor@ijsat.org

Structural, Morphological and Compositional Analysis of WS_2 thin films

Chetan R. Yewale[1], Rajendra V. Wagh[2], Vaishali T. Salunke[3], Arun V. Patil[4], Satish S. Mandawade[5]

[1,4]Department of Physics and Research Centre, MGV's MSG Arts, Science and Commerce College, Malegaon, Dist: Nashik, Maharashtra, India
[2]MVP's Arts, Commerce and Science College, Nandgaon, At-Post- Nandgaon Dist: Nashik, Maharashtra, India
[3]Department of Electronic Science, MGV's MSG Arts, Science and Commerce College, Malegaon, Dist: Nashik, Maharashtra, India
[4]Department of Physics, MGV's, Arts, Science and Commerce College, Nimgaon, Dist. Nashik, Maharashtra, India
[5]Department of Physics and Research Centre, MGV's MSG Arts, Science and Commerce College, Malegaon, Dist. Nashik, Affiliated to Savitribai Phule Pune University, Maharashtra, India

Abstract:
Tungsten disulfide (WS_2) thin films were prepared using a sol–gel-assisted spin-coating technique for structural, morphological, and compositional investigation. Tungsten- and sulfur-based precursors were used to prepare the precursor solution, which was deposited on the substrate at 1000 rpm for 60 s. The deposited films were subjected to thermal treatment at 400 °C for 3 h in a closed muffle furnace. The structural characteristics of the prepared WS_2 thin films were investigated using X-ray diffraction (XRD), while surface morphology and elemental composition were examined using scanning electron microscopy (SEM) and energy-dispersive X-ray spectroscopy (EDX) respectively. XRD analysis confirmed the crystalline nature of the deposited film, with the observed diffraction features corresponding to the WS_2 crystalline phase. The crystallite size calculated using the Debye–Scherrer equation was 90.91 nm. SEM analysis revealed a rough, granular, and porous surface morphology comprising nanoscale grains with intergranular voids and localized agglomeration. EDX analysis confirmed the presence of tungsten and sulfur along with oxygen. The combined structural, morphological and compositional results establish the characteristics of the prepared WS_2 thin-film system and provide a basis for its investigation in surface-dependent electronic and sensing applications.

Keywords: WS_2 thin films; sol–gel; spin coating; crystallite size; surface morphology; tungsten disulfide.

1. Introduction

The development of advanced functional materials with controlled structural, morphological, electrical, and surface properties has attracted considerable attention for next-generation electronic, sensing, energy, and optoelectronic technologies [1, 2]. Among the family of transition-metal dichalcogenides (TMDs), tungsten disulfide (WS_2) has emerged as an important layered semiconductor because of its distinctive

crystal structure, thickness-dependent electronic properties, high surface-to-volume ratio, chemical stability, and strong interaction with electromagnetic radiation [2-4]. WS_2 belongs to the MX_2 class of TMDs, in which a tungsten (W) atomic layer is sandwiched between two sulfur (S) atomic layers. Within an individual S–W–S layer, strong W–S bonding maintains the structural framework, whereas adjacent layers interact through weak van der Waals forces. This layered configuration produces an anisotropic material structure and facilitates the formation of thin films, nanosheets, and few-layer structures [5, 6].

WS_2 exhibits several polymorphic forms, among which the semiconducting 2H phase is particularly important for electronic and sensing applications. The 2H phase possesses a hexagonal structure and consists of trigonal-prismatic coordination around the tungsten atoms. The electronic structure of WS_2 is strongly dependent on the number of layers. Bulk and multilayer WS_2 exhibit an indirect band-gap transition, whereas reduction toward the monolayer regime produces a direct band gap of approximately 2 eV [6, 7]. This thickness-dependent electronic structure is accompanied by strong excitonic effects, high carrier mobility, substantial light absorption, and pronounced light–matter interaction. These characteristics have established WS_2 as an important material for field-effect transistors, photodetectors, light-emitting devices, memory devices, optical modulators, and different sensing platforms [7-9]. The structural characteristics of WS_2 strongly influence its functional performance. Crystal phase, crystallinity, crystallite dimensions, lattice arrangement, defects, grain boundaries, and preferential orientation determine charge transport and surface-related interactions. In thin-film systems, grain size and intergranular regions are particularly significant because they control the density of active surface sites and pathways for charge transport. A nanostructured WS_2 surface containing interconnected grains and surface voids provides an increased accessible surface area for adsorption and interfacial reactions. Defect sites, sulfur vacancies, and edge sites further modify the electronic structure and surface reactivity of WS_2. Recent studies have highlighted defect engineering and controlled incorporation of impurities as important approaches for tailoring the electrical and optoelectronic characteristics of WS_2 [10, 11].

The preparation method plays an important role in controlling the structural and morphological characteristics of WS_2 thin films. Various techniques have been investigated, including chemical deposition, sputtering followed by sulfurization, chemical vapor deposition, hydrothermal synthesis, and other solution-based approaches. Vapor-phase techniques provide effective control over layer thickness and crystalline quality, while solution-based methods offer relatively simple processing and compatibility with large-area deposition [12, 13]. Earlier investigations demonstrated the formation of crystalline WS_2 thin films through chemical deposition, while more recent studies have focused on controlled growth of layered WS_2 films and nanosheets. The selection of deposition parameters such as precursor chemistry, concentration, substrate condition, deposition rate, spinning speed, thermal treatment, and atmosphere directly influences nucleation, grain growth, phase formation, and surface morphology [14, 15]. Among solution-processing approaches, the sol–gel-assisted spin-coating technique provides a simple route for producing uniform thin films with controlled deposition conditions. In this method, tungsten- and sulfur-containing precursors are converted into a homogeneous precursor solution, followed by deposition onto a suitable substrate through controlled spinning [16, 17]. The centrifugal force generated during spin coating distributes the precursor over the substrate surface and determines the initial film thickness and uniformity. Parameters such as spinning speed and coating duration influence solvent evaporation, precursor distribution, nucleation density, and the resulting film morphology. Subsequent thermal

treatment promotes solvent removal, decomposition of precursor species, diffusion of constituent atoms, and development of the crystalline phase. WS_2 is also of considerable interest for sensing applications because its layered structure provides a large exposed surface and abundant adsorption sites. Gas molecules interacting with the WS_2 surface modify the local charge distribution and carrier concentration, producing measurable changes in electrical conductivity or resistance. Surface defects, grain boundaries, and edge sites influence the adsorption and desorption processes and therefore affect sensor response and recovery characteristics [14-16]. WS_2-based materials have been investigated for the detection of gases and other environmental species, including through composite structures with metal oxides and carbon-based materials. Despite extensive research on two-dimensional WS_2, the relationship between the deposition conditions, crystalline structure, surface morphology, and elemental composition of solution-processed WS_2 thin films requires systematic investigation [16-18]. In particular, understanding the surface morphology and elemental composition after thermal treatment is important because oxygen-containing species and surface oxidation influence the chemical and electronic characteristics of WS_2. Therefore, the present work focuses on the preparation and characterization of WS_2 thin films using a sol–gel-assisted spin-coating technique.

2. Material and method

2.1 Synthesis and development of WS_2 thin films

WS_2 thin films were prepared using a sol–gel-assisted spin-coating technique. Analytical-grade sodium tungstate (Na_2WO_4, 0.25 M) and sodium thiosulfate ($Na_2S_2O_3$, 0.25 N) were used as tungsten and sulfur precursors respectively. Double-distilled water was used as the solvent, and citric acid ($C_6H_8O_7$, 1 M) was incorporated as a complexing agent to improve the homogeneity and stability of the precursor sol. 10 mL of Na_2WO_4, 20 mL of $Na_2S_2O_3$, 5 mL of citric acid, and 5 mL of 25% hydrazine hydrate were mixed under continuous stirring, and the final volume was adjusted to 100 mL using double-distilled water [19, 20]. The resulting homogeneous sol was deposited onto cleaned glass substrates by spin coating at 1000 rpm for 60 s and dried under an IR lamp. The coated films were subsequently annealed at 400 °C for 3 h in a closed muffle furnace to promote crystallization and formation of the WS_2 thin-film structure [20, 21]. The prepared films were characterized using XRD, SEM and EDX to investigate their structural, morphological and elemental characteristics.

3. Result and Discussion

3.1 Scanning Electron Microscopy

Figure 1(a–d) presents the SEM micrographs of the WS_2 thin film recorded at different magnifications of 1000×, 3000×, 5000× and 10,000× respectively. At 1000× [Fig. 1(a)], the surface exhibits a continuous and highly textured morphology consisting of fine particles distributed across the substrate, together with several interconnected voids [22, 23]. The higher-magnification image at 3000× [Fig. 1(b)] reveals a dense population of nanosized grains with noticeable intergranular spaces and localized agglomeration. At 5000× [Fig. 1(c)], the individual WS_2 particles become more clearly distinguishable, with numerous fine grains surrounding relatively larger agglomerated regions [24, 25]. The 10,000× image [Fig. 1(d)] provides clear evidence of nanoscale granular features and interconnected surface gaps. The presence of these interparticle voids and rough surface features increases the accessible surface area of the film and provides a larger number of active sites for surface adsorption, which is particularly important for gas-sensing applications. The progressive appearance of smaller grains at higher magnification indicates a

heterogeneous nanostructured surface with a high density of grain boundaries [21-25]. Such grain boundaries provide preferential sites for interaction between the WS_2 surface and adsorbed gas molecules, thereby influencing the electrical resistance and sensing response of the film.

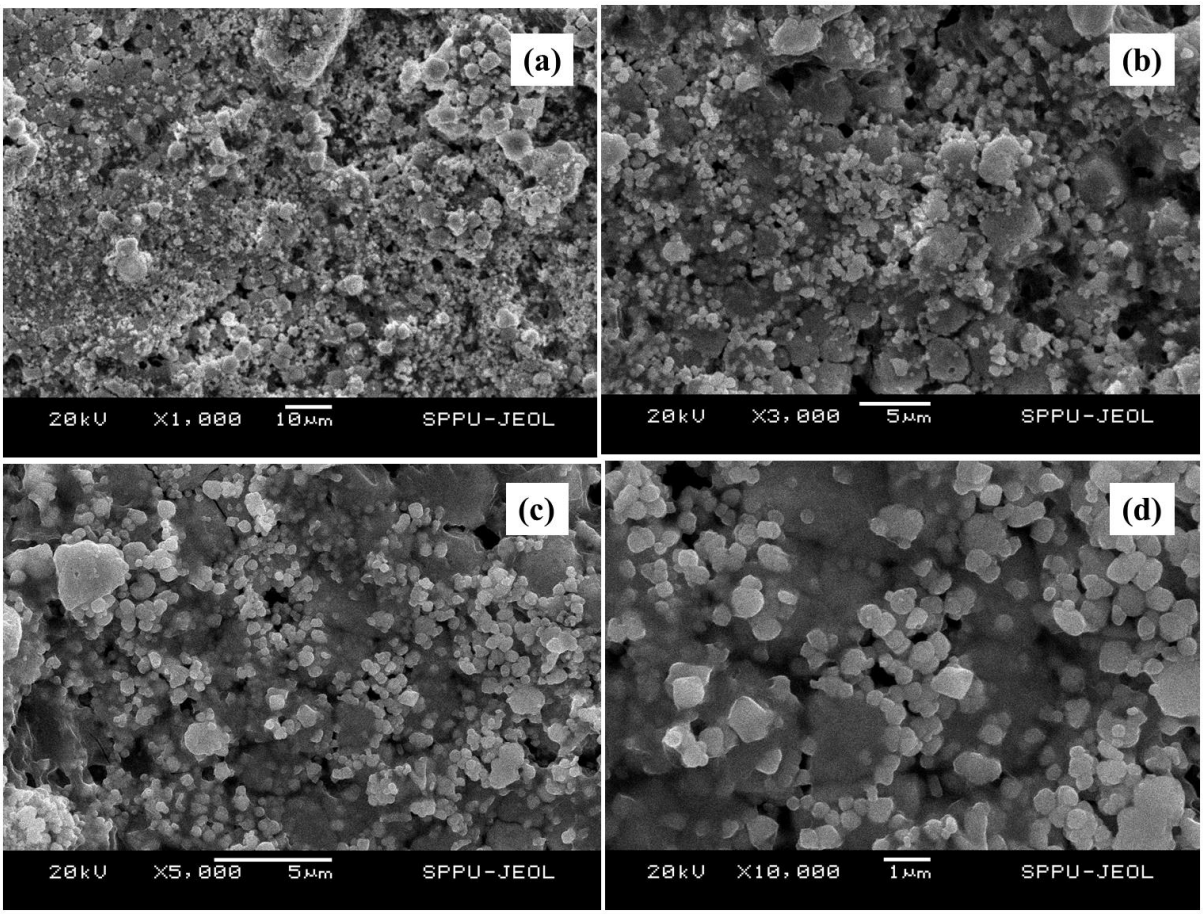

Figure 1 (a-d): SEM micrograph of WS_2 thin films at different magnifications

3.2 Energy-dispersive X-ray spectroscopy

Figure 2 presents the EDX spectrum of the prepared WS_2 thin film, while the corresponding elemental composition is summarized in Table 1. Distinct characteristic peaks associated with tungsten (W), sulfur (S) and oxygen (O) are observed in the spectrum, confirming the presence of these elements within the analyzed film [26, 27]. The quantitative EDX analysis gives 40.07 wt.% W, 11.45 wt.% S, and 48.48 wt.% O, corresponding to 6.05 at.% W, 9.90 at.% S, and 84.05 at.% O respectively. The tungsten and sulfur signals verify the incorporation of the principal constituent elements of WS_2 in the deposited film. The relatively high oxygen content requires consideration of the thermal processing conditions [28, 29]. The films were annealed at 400 °C for 3 h in a closed muffle furnace. At 400 °C, surface oxidation of WS_2 produces oxygen-containing tungsten species, while oxygen adsorption and incorporation at surface defects and grain boundaries also contribute to the measured oxygen signal.

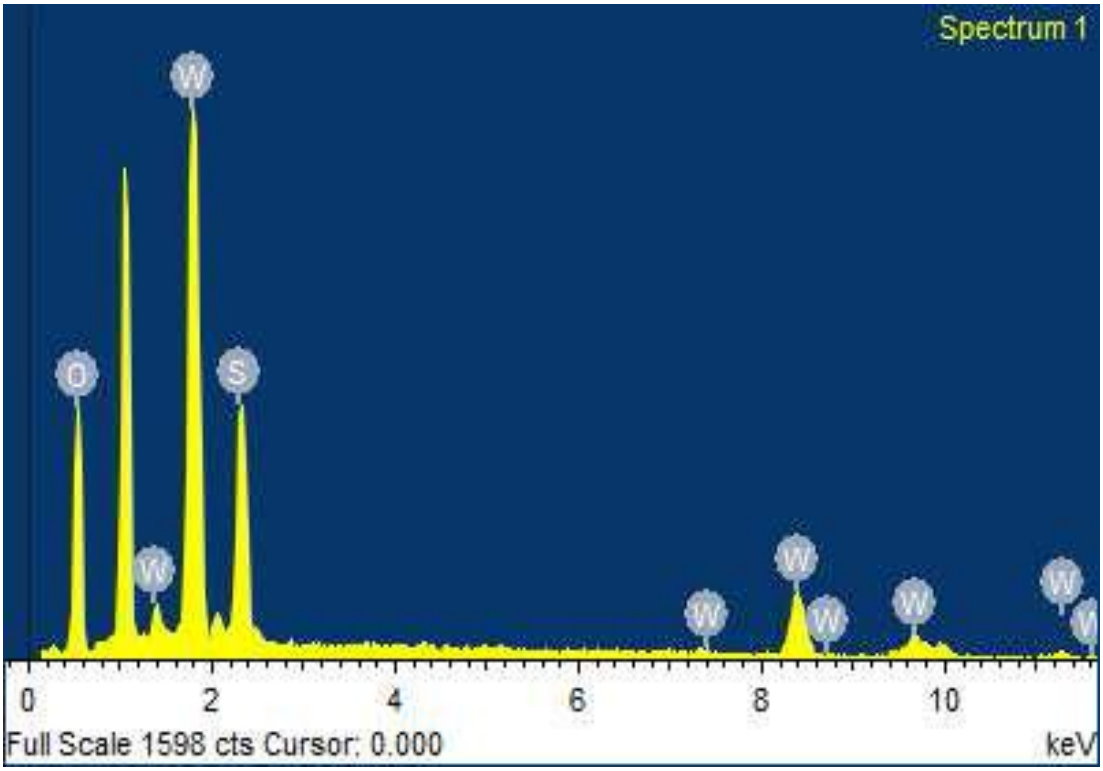

Figure 2: EDX spectra of WS_2 thin films

Table 1. EDX elemental composition of WS_2 thin film

Element	Weight %	Atomic %
O	48.48	84.05
S	11.45	9.90
W	40.07	6.05
Total	100.00	100.00

EDX probes a finite interaction volume, so oxygen-containing species from the substrate or surface layer can contribute to the measured composition depending on the film thickness and electron-beam penetration depth. Thus, the oxygen signal is associated with the thermal treatment environment, surface oxidation, and possible substrate contribution, rather than being attributed exclusively to WS_2 itself. The EDX spectrum does not show evidence of additional metallic elements, indicating that W and S constitute the principal elements of the WS_2-derived film [30, 31]. The observed elemental composition, together with the structural and morphological characterization, provides evidence for the formation of a tungsten–sulfur-based thin-film system with a significant oxygen-containing surface or near-surface component.

3.3 X-ray diffraction

Figure 3 shows the XRD pattern of the prepared WS_2 thin film recorded over the 2θ range of 10–80°. The diffraction pattern exhibits several well-defined reflections, indicating the crystalline nature of the deposited film. The characteristic reflections of hexagonal 2H-WS_2 are reported in the literature at approximately 14.3°, 28.9°, 32.8–33.6°, 39.5°, 43.9°, 49.6°, 58.4–60° and higher angles, which are indexed to the (002), (004), (100), (101), (103), (006), (105) and (008) planes respectively, according to

JCPDS Card No. 08-0237 [32, 33]. The 2H-WS_2 phase possesses a hexagonal structure with $P6_3/mmc$ space group. The intense (002) reflection near 14.3° represents the characteristic basal-plane reflection of layered WS_2 and indicates preferential orientation along the c-axis when it dominates the diffraction pattern.

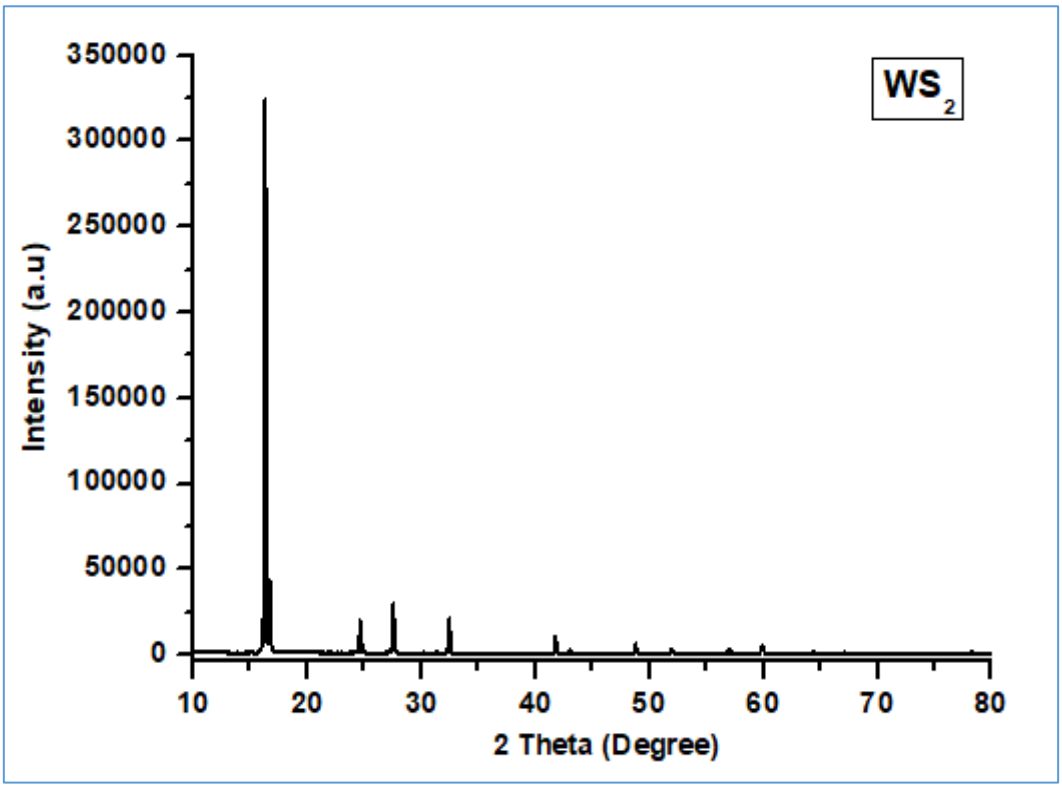

Figure 3: XRD pattern of WS_2 thin films

The crystallite size of the WS_2 thin film was calculated from the full width at half maximum (FWHM) of the principal diffraction peak using the Debye–Scherrer equation 1 [34],

$$D=K\lambda/\beta\cos\theta \qquad \text{Eq.1.}$$

Where,

D is the crystallite size, Kis the shape factor (0.9), λ is the wavelength of Cu Kα radiation (0.15406 nm), β is the FWHM of the diffraction peak in radians, and θ is the corresponding Bragg angle.

For the WS_2 thin film, the measured FWHM was 0.1032°, which corresponds to approximately 0.001802 rad. Using the corresponding diffraction angle, the calculated crystallite size was 90.91 nm. The relatively narrow FWHM indicates well-developed crystalline domains and comparatively low peak broadening [29, 31]. The calculated crystallite size represents the average coherent diffraction-domain size rather than the physical particle or grain size observed in SEM. The large crystallite size is consistent with the distinct and sharp diffraction features observed in the XRD pattern, whereas the SEM micrograph shows nanoscale surface grains and agglomerated regions [34-36]. Thus, the XRD and SEM results describe different structural length scales: XRD provides the average coherent crystalline-domain size, while SEM provides information about surface morphology and grain/agglomerate features.

Conclusions

WS_2 thin films were successfully synthesized using a sol–gel-assisted spin-coating technique employing sodium tungstate and sodium thiosulfate as tungsten and sulfur precursors, respectively. The films were deposited at 1000 rpm for 60 s and annealed at 400 °C for 3 h in a closed muffle furnace. XRD analysis confirmed the crystalline nature of the prepared WS_2 thin film, with a FWHM of 0.1032° and an average crystallite size of 90.91 nm calculated using the Debye–Scherrer equation. SEM analysis revealed a textured granular surface with nanoscale grains, intergranular voids, and agglomerated regions, providing a high density of surface-active sites. EDX analysis confirmed the presence of W, S and O, with the oxygen signal associated with the oxygen-containing thermal environment and surface oxidation during annealing. The combined structural, morphological, and compositional results demonstrate the successful development of a crystalline WS_2-based thin-film system with a textured surface suitable for further investigation in gas-sensing, electronic, and surface-dependent applications.

Acknowledgment

The authors are thanks to the Department of Physics and research centre, MGV's arts, Science and Commerce College, Malegaon, Maharashtra, India for providing laboratory facilities for the current research work. The author also thanks the Department of Physics, SPPU, Pune, India for providing the facilities for SEM, EDS and XRD characterizations facilities.

REFERENCES:

1. Cao, S., Liu, T., Hussain, S., Zeng, W., Zhang, Y., Wang, X. and others, 2014. Hydrothermal synthesis of variety low dimensional WS_2 nanostructures. Materials Letters, 129, pp.205–208.
2. Ennaoui, A., Fiechter, S., Ellmer, K., Scheer, R. and Diesner, K., 1995. Preparation of textured and photoactive 2H-WS_2 thin films by sulfurization of WO_3. Thin Solid Films, 261, pp.124–131.
3. Schmidt, P., Schmalz, K., Fröhlich, H. and others, 1992. Preparation and microstructure WS_2 thin films. Thin Solid Films, 217, pp.91–97.
4. Stanić, V., Dimitrijević, R. and others, 1997. Preparation of tungsten sulfides by sol–gel processing. Journal of Non-Crystalline Solids.
5. Gourmelon, E., Rigoult, J., Portemer, F., Ouvrard, G. and Grenier, J.C., 1997. Preparation and characterization of tungsten disulfide thin films. Solar Energy Materials and Solar Cells.
6. Regula, M., Lignier, O., Meunier, F. and others, 1996. Preparation and characterization of tungsten disulfide thin films. Thin Solid Films.
7. Gourmelon, E., Lignier, O., Portemer, F., Ouvrard, G. and Grenier, J.C., 1997. Optical and structural properties of tungsten disulfide thin films. Solar Energy Materials and Solar Cells.
8. Rathod, U.P., Patel, M.K. and others, 2019. Growth of pulsed laser deposited few-layer WS_2 films. Journal of Vacuum Science & Technology A.
9. Hotovy, I., Spiess, L., Sojkova, M.V., Kostic, I., Mikolasek, M., Predanocy, M., Romanus, H., Hulman, M. and Rehacek, V., 2018. Structural and optical properties of WS_2 prepared using sulfurization of different thick sputtered tungsten films. Applied Surface Science, 461, pp.133–138.
10. Hotovy, I., Spiess, L., Mikolasek, M., Kostic, I., Sojkova, M., Romanus, H., Hulman, M., Buc, D. and Rehacek, V., 2021. Layered WS_2 thin films prepared by sulfurization of sputtered W films. Applied Surface Science, 548, 148719.

11. Hussain, S. and Dam, S., 2021. Synthesis of vertically stacked, highly oriented WS_2 thin films by electron beam evaporation. Thin Solid Films, 734, 138851.
12. Kim, J., Byun, S., Lee, J., Choi, J., Lee, H. and others, 2018. Growth and characterization of WS_2 thin films for electronic applications. Applied Surface Science.
13. Yeo, S., Nandi, D.K., Rahul, R., Kim, T.H., Shong, B., Jang, Y., Bae, J.S., Han, J.W., Kim, S.H. and Kim, H., 2018. Low-temperature direct synthesis of high quality WS_2 thin films by plasma-enhanced atomic layer deposition for energy related applications. Applied Surface Science, 459, pp.596–605.
14. Song, J.G., Park, J., Lee, W., Choi, T., Jung, H.S. and others, 2013. Layer-controlled, wafer-scale, and conformal synthesis of tungsten disulfide nanosheets using atomic layer deposition. ACS Nano, 7, pp.11333–11340.
15. Zeng, W., Wang, J., Chen, Z. and others, 2018. Layer-controlled and atomically thin WS_2 films prepared by sulfurization of atomic-layer-deposited WO_3 films. Journal of Alloys and Compounds, 745, pp.834–839.
16. Lan, F., Wang, R., Xu, S. and others, 2020. Controllable synthesis of millimeter-size single crystal WS_2. Applied Surface Science.
17. Xu, Z., Lv, Y., Li, J., Huang, F., Nie, P., Zhang, S., Zhao, S., Zhao, S. and Wei, G., 2019. CVD controlled growth of large-scale WS_2 monolayers. RSC Advances, 9, pp.29628–29635.
18. Lin, Y.C., Yeh, C.H., Lin, H.C., Siao, M.D., Liu, Z., Nakajima, H., Okazaki, T., Chou, M.Y., Suenaga, K. and Chiu, P.W., 2018. Stable 1T tungsten disulfide monolayer and its junctions: growth and atomic structures. ACS Nano, 12, pp.12080–12088.
19. Mak, K.F., Lee, C., Hone, J., Shan, J. and Heinz, T.F., 2010. Atomically thin MoS_2: a new direct-gap semiconductor. Physical Review Letters, 105, 136805.
20. Radisavljevic, B., Radenovic, A., Brivio, J., Giacometti, V. and Kis, A., 2011. Single-layer MoS_2 transistors. Nature Nanotechnology, 6, pp.147–150.
21. Schwierz, F., 2010. Graphene transistors. Nature Nanotechnology, 5, pp.487–496.
22. Wang, Q.H., Kalantar-Zadeh, K., Kis, A., Coleman, J.N. and Strano, M.S., 2012. Electronics and optoelectronics of two-dimensional transition metal dichalcogenides. Nature Nanotechnology, 7, pp.699–712.
23. Chhowalla, M., Shin, H.S., Eda, G., Li, L.J., Loh, K.P. and Zhang, H., 2013. The chemistry of two-dimensional layered transition metal dichalcogenide nanosheets. Nature Chemistry, 5, pp.263–275.
24. Manzeli, S., Ovchinnikov, D., Pasquier, D., Yazyev, O.V. and Kis, A., 2017. 2D transition metal dichalcogenides. Nature Reviews Materials, 2, 17033.
25. Lan, C., Li, C., Ho, J.C. and Liu, Y., 2021. 2D WS_2: From vapor phase synthesis to device applications. Advanced Electronic Materials, 7, 2000688.
26. Li, C., Sang, D., Ge, S., Zou, L. and Wang, Q., 2024. Recent excellent optoelectronic applications based on two-dimensional WS_2 nanomaterials: a review. Molecules, 29, 3341.
27. Kumar, A., Mirzaei, A., Lee, M.H., Ghahremani, Z., Kim, T.U., Kim, J.Y., Kwoka, M., Kumar, M., Kim, S.S. and Kim, H.W., 2024. Strategic review of gas sensing enhancement ways of 2D tungsten disulfide/selenide-based chemiresistive sensors: decoration and composite. Journal of Materials Chemistry A, 12, pp.3771–3806.
28. Bhattacharyya, P. and Acharyya, D., 2021. Impact of device configurations on sensing performance of WS_2-based gas sensors: a review. IEEE Sensors Journal, 21, pp.22414–22425.

29. Järvinen, T., Lorenz, M., Österlund, L. and others, 2019. WS_2 and MoS_2 thin film gas sensors with high response to NH_3 in air at low temperature. Nanotechnology.
30. Li, Y., Chen, D., Xia, F., Tan, J.Z.Y., Song, J., Song, W. and Caruso, R.A., 2016. Flowerlike WSe_2 and WS_2 microspheres: one-pot synthesis, formation mechanism and application in heavy metal ion sequestration. Chemical Communications, 52, pp.4481–4484.
31. Ling, Y., Yang, Z., Zhang, Q., Zhang, Y., Cai, W. and Cheng, H., 2018. A self-template synthesis of defect-rich WS_2 as a highly efficient electrocatalyst for the hydrogen evolution reaction. Chemical Communications, 54, pp.2631–2634.
32. Zhu, S.Q., Xu, C., Li, M.Y., He, C.S., Ye, J.C. and Li, X., 2025. WS_2-based gas sensors: strategies for performance optimization and emerging trends. Microchemical Journal, 218, 115655.
33. Cao, S., Liu, T., Hussain, S., Zeng, W. and others, 2014. Synthesis and characterization of novel chrysanthemum-like tungsten disulfide (WS_2) nanostructure: structure, growth and optical absorption property. Journal of Materials Science: Materials in Electronics, 26, pp.809–814.
34. Cabeda, D.S., Rolim, G.K., Soares, G.V., Andrade, A.M.H. and Radtke, C., 2023. Timing of sulfur introduction in the sulfurization of WO_3 films dictates WS_2 formation. Applied Surface Science, 610, 155488.
35. Gatensby, R., et al., 2016. Investigations of vapour-phase deposited transition metal dichalcogenide films for future electronic applications. Solid-State Electronics.
36. Ng, S.M., et al., 2016. WS_2 nanotube formation by sulphurization: effect of precursor tungsten film thickness and stress. Materials Chemistry and Physics.